

# Test–Retest Repeatability of [<sup>18</sup>F]MC225-PET in Rodents: A Tracer for Imaging of P-gp Function

Lara García-Varela, David Vázquez García, Manuel Rodríguez-Pérez, Aren van Waarde, Jürgen W. A. Sijbesma, Anna Schildt, Chantal Kwizera, Pablo Aguiar, Tomás Sobrino, Rudi A. J. O. Dierckx, Philip H. Elsinga, and Gert Luurtsema\*

Cite This: *ACS Chem. Neurosci.* 2020, 11, 648–658

Read Online

ACCESS |

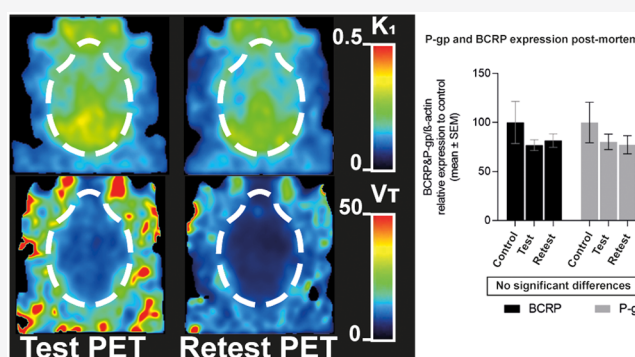
Metrics & More

Article Recommendations

Supporting Information

**ABSTRACT:** In longitudinal PET studies, animals are repeatedly anesthetized which may affect the repeatability of PET measurements. The aim of this study was to assess the effect of anesthesia on the P-gp function as well as the reproducibility of [<sup>18</sup>F]MC225 PET scans. Thus, dynamic PET scans with blood sampling were conducted in 13 Wistar rats. Seven animals were exposed to isoflurane anesthesia 1 week before the PET scan (“Anesthesia-exposed” PET). A second group of six animals was used to evaluate the reproducibility of measurements of P-gp function at the blood–brain barrier (BBB) with [<sup>18</sup>F]MC225. In this group, two PET scans were made with a 1 week interval (“Test” and “Retest” PET). Pharmacokinetic parameters were calculated using compartmental models and metabolite-corrected plasma as an input function. “Anesthesia-exposed” animals showed a 28% decrease in whole-brain volume of distribution ( $V_T$ ) ( $p < 0.001$ ) compared to “Test”, where the animals were not previously anesthetized. The  $V_T$  at “Retest” also decreased (19%) compared to “Test” ( $p < 0.001$ ). The  $k_2$  values in whole-brain were significantly increased by 18% in “Anesthesia-exposed” ( $p = 0.005$ ) and by 15% in “Retest” ( $p = 0.008$ ) compared to “Test”. However, no significant differences were found in the influx rate constant  $K_1$ , which is considered as the best parameter to measure the P-gp function. Moreover, Western Blot analysis did not find significant differences in the P-gp expression of animals not pre-exposed to anesthesia (“Test”) or pre-exposed animals (“Retest”). To conclude, anesthesia may affect the brain distribution of [<sup>18</sup>F]MC225 but it does not affect the P-gp expression or function.

**KEYWORDS:** Anesthesia, blood-brain barrier, isoflurane, P-glycoprotein, positron emission tomography, preclinical studies, test–retest repeatability



## 1. INTRODUCTION

Delivery of many drugs to the central nervous system (CNS) is reduced by the action of efflux transporters in the blood–brain barrier (BBB), such as the breast cancer resistance protein (BCRP), and particularly P-glycoprotein (P-gp), i.e., ABCB1.<sup>1</sup> This transporter is known to limit the brain entry of antipsychotics, antidepressants, antiepileptic drugs, and chemotherapeutic agents.<sup>2</sup> Several structurally diverse compounds act as substrates or modulators of P-gp. The transporter is, therefore, involved in drug–drug interactions (DDI) at the BBB with corresponding alterations of drug concentration, decreases in therapeutic efficacy and increases of toxicity.<sup>3,4</sup> For this reason, the U.S. Food and Drug Administration (FDA) and European Medicines Agency (EMA) have developed specific guidelines for the screening of new drugs in order to determine their potential interactions with P-gp.<sup>5,6</sup>

In vitro screening is based on simplified models of the living system, positron emission tomography (PET) imaging of the mammalian brain may provide important information con-

cerning P-gp mediated drug transport and the mechanism underlying DDIs. Several PET tracers are available for this purpose, such as (R)-[<sup>11</sup>C]Verapamil and [<sup>11</sup>C]N-desmethyl-loperamide.<sup>7,8</sup> Recently, [<sup>18</sup>F]MC225 (5-(1-(2-[<sup>18</sup>F]-fluoroethoxy))-[3-(6,7-dimethoxy-3,4-dihydro-1H-isoquinolin-2-yl)-propyl]-5,6,7,8-tetrahydronaphthalene) was developed and validated for quantitative imaging of P-gp.<sup>9,10</sup> This tracer is classified as a weak substrate of P-gp, resulting in higher brain uptake of radioactivity at baseline compared to other imaging agents.<sup>10</sup> Inhibitors of P-gp were shown to increase the cerebral uptake of [<sup>18</sup>F]MC225.<sup>10</sup>

Since PET imaging is minimally invasive, this technique seems well-suited for longitudinal studies, e.g. the scanning of a

Received: December 20, 2019

Accepted: January 21, 2020

Published: January 21, 2020

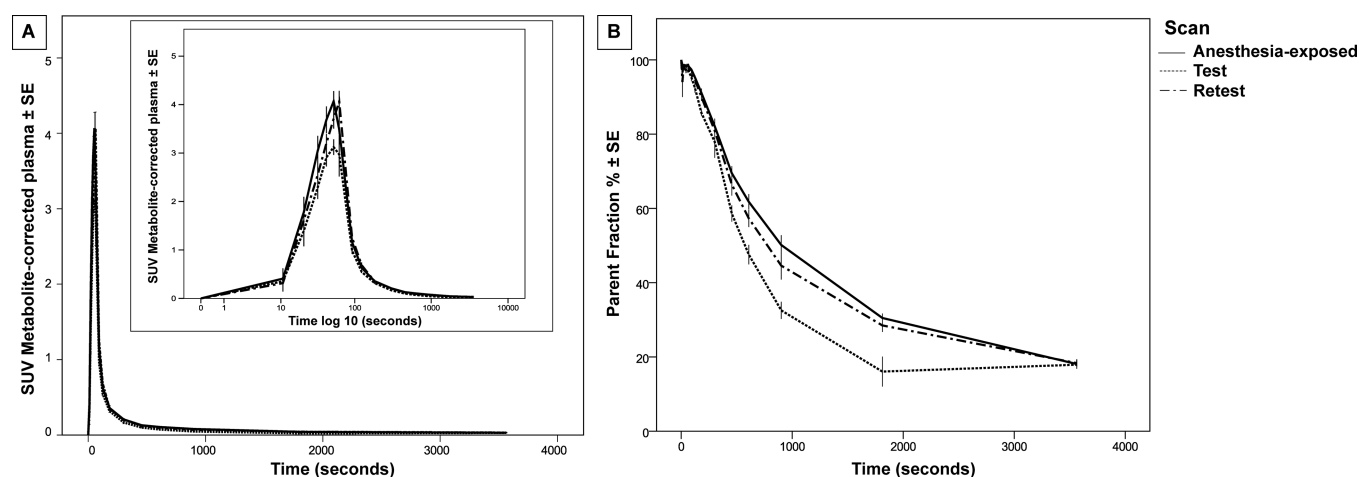


**Figure 1.**  $[^{18}\text{F}]\text{MC225}$  concentration over the time course of the different PET scans: (A) metabolite-corrected time–activity curves in plasma and (B) percentage of parent fraction as a function of time. Data are plotted as  $\text{EMM} \pm \text{SE}$ .

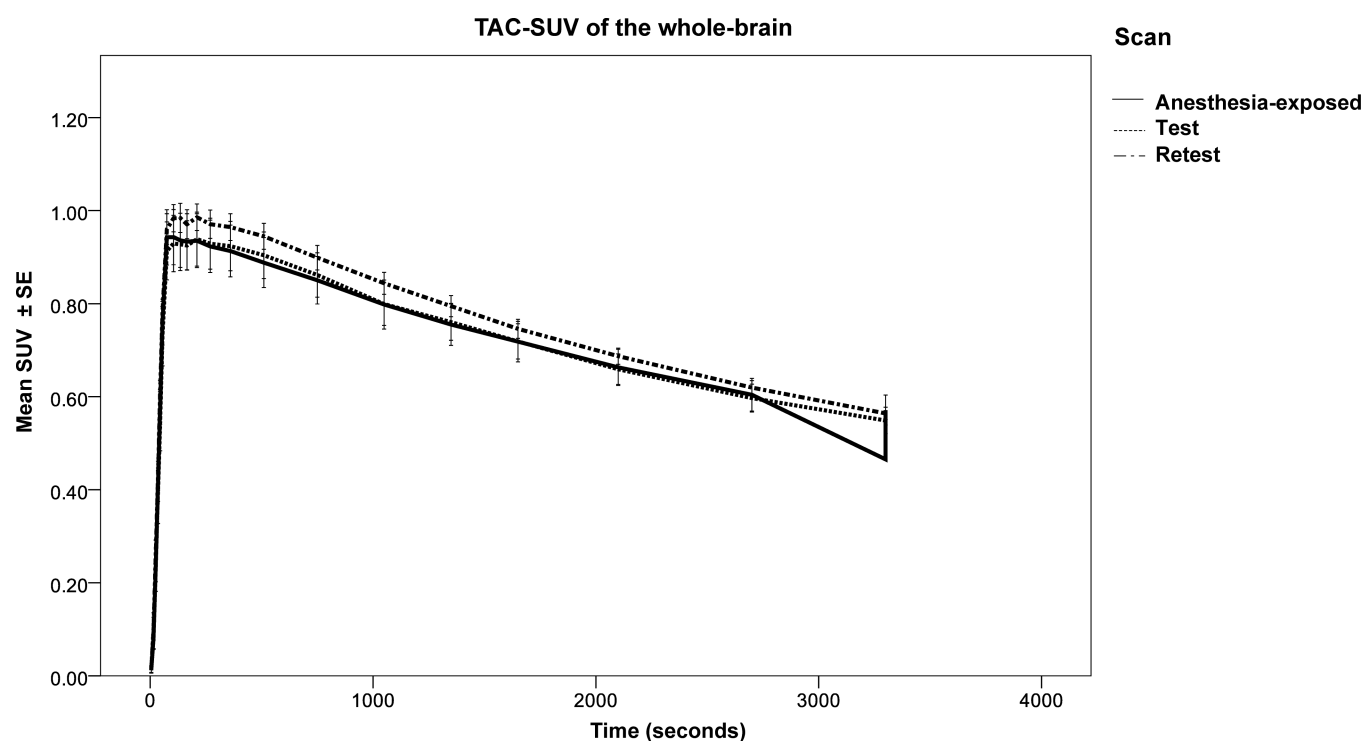


**Figure 2.** Whole-brain TACs of  $[^{18}\text{F}]\text{MC225}$  at the three different scans.

subject at baseline and after various interventions. However, PET imaging of small animals involves the use of anesthesia in order to immobilize the subject during the scan. Since it is well-known that anesthesia may affect the distribution of tracers in the CNS,<sup>3,11,12</sup> it is important to examine the impact of anesthesia on the brain uptake of P-gp tracers. Moreover, the reproducibility of  $[^{18}\text{F}]\text{MC225}$  PET scans should be assessed before longitudinal studies with this tracer can be performed.

The present study aimed to assess the influence of previous exposure to isoflurane anesthesia on P-gp function at the BBB and the reproducibility of  $[^{18}\text{F}]\text{MC225}$  PET scans in rats. Pharmacokinetic parameters, such as the volume of distribution ( $V_T$ ) and the rate constants ( $K_1$  and  $k_2$ ) of  $[^{18}\text{F}]\text{MC225}$ , were calculated using compartmental models and metabolite-corrected plasma radioactivity as input function. Western Blot

(WB) analysis was performed to assess the expression of P-gp and BCRP transporters at the BBB.

## 2. RESULTS AND DISCUSSION

PET imaging can provide insight into the physiology and pathophysiology of living brains.<sup>13</sup> Moreover, it is a non-invasive technique that allows the monitoring of animals in longitudinal studies at several time points, before and after the onset of disease or treatment. Thus, each animal can serve as its own control, which reduces intersubject variability.<sup>14</sup> However, many factors may interfere with molecular mechanisms inside the brain and may have a negative impact on PET measurements. These include gender and strain differences of physiology and metabolism, the age of the animals, the composition of the diet or the duration of the fasting, the circadian rhythm and, the dose and kind of

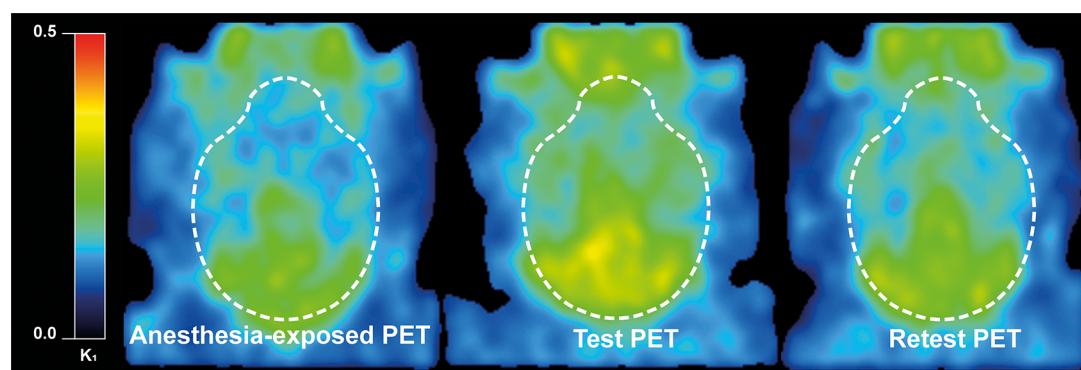


**Figure 3.** Parametric images of representative PET scans (Anesthesia-exposed, Test, and Retest) showing voxel-wise values for  $K_1$  of  $[^{18}\text{F}]\text{MC225}$  calculated by ITCM.

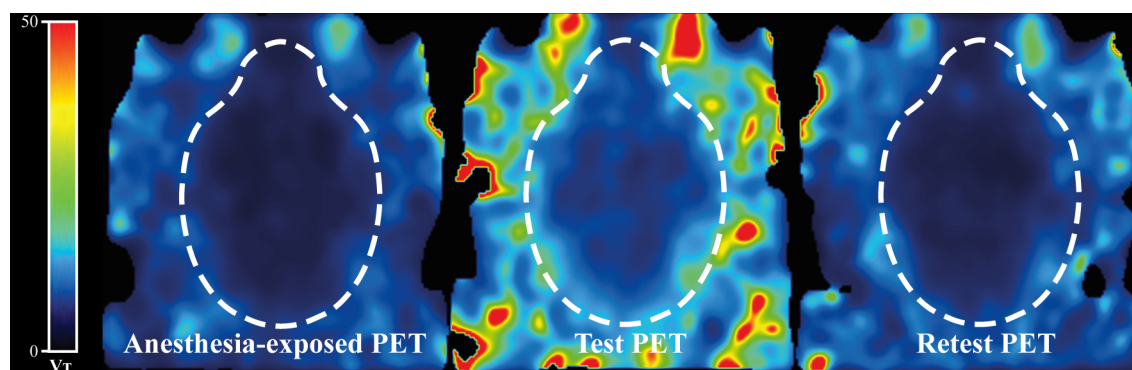


**Figure 4.** Parametric images of representative PET scans (Anesthesia-exposed, Test, and Retest) showing voxel-wise values for  $V_T$  of  $[^{18}\text{F}]\text{MC225}$  calculated by ITCM.

anesthetic.<sup>11</sup> Therefore, the reproducibility of PET scans with a novel tracer should be evaluated before longitudinal studies are performed. Since anesthesia is commonly used to immobilize animals during acquisition of PET data, animals are repeatedly anesthetized in each longitudinal study design. Thus, it is necessary to examine the effect of anesthesia on the imaging target (in this case, cerebral P-gp function). To this aim, dynamic PET scans with  $[^{18}\text{F}]\text{MC225}$  and blood sampling were made in 13 healthy male Wistar rats. In order to test the effect of the anesthesia on the P-gp function, seven animals were exposed to isoflurane anesthesia 1 week before the PET scan (“Anesthesia-exposed” PET). A second group of six animals was used to evaluate the reproducibility of measurements of P-gp function at the BBB with  $[^{18}\text{F}]\text{MC225}$ . In this group, two PET scans were made with a 1 week interval (“Test” and “Retest” PET).

**2.1. Results.** **2.1.1. Tracer Production.** The tracer was obtained in an average synthesis time of  $92 \pm 7$  min (mean  $\pm$  SD) with a radiochemical yield of  $4.9 \pm 0.9\%$  (decay-corrected). The radiochemical purity of  $[^{18}\text{F}]\text{MC225}$  was higher than 99%, and the molar activity was higher than 29 TBq/mmol.

**2.1.2. Plasma Kinetics and Metabolism of  $[^{18}\text{F}]\text{MC225}$ .** Since the tracer was injected during a period of 1 min using a Harvard infusion pump, the concentration of  $[^{18}\text{F}]\text{MC225}$  peaked at 62 s after the start of tracer injection in metabolite-corrected plasma time–activity curves (TACs).

Statistical analysis revealed that the plasma concentration of  $[^{18}\text{F}]\text{MC225}$  (corrected for metabolites) was significantly higher in “Anesthesia-exposed” and “Retest” scans compared to “Test”. Figure 1A indicates a sharper rise of  $[^{18}\text{F}]\text{MC225}$  in

“Anesthesia-exposed” and “Retest” scans compared to “Test”. The parent fraction in plasma was also higher in “Anesthesia-exposed” and “Retest” scans than in “Test”, as can be observed in Figure 1B. Table 1 in the Supporting Information shows the estimated marginal means (EMM) and standard errors (SE) calculated by generalized estimated equation (GEE) analysis, and the statistical significance of differences between scans.

However, we did not observe any statistically significant differences in the biological half-life ( $T_{1/2}$ ) of the tracer in the three scans (Anesthesia-exposed, Test, and Retest).

**2.1.3. Brain Kinetics of  $[^{18}\text{F}]\text{MC225}$ .** **2.1.3.1. The SUV-TAC of the Whole Brain.** Whole-brain TACs are shown in Figure 2. Although standardized uptake values (SUVs) seem higher in the “Retest” group than in the other two groups, the statistical analysis did not indicate any significant differences between “Anesthesia-exposed” and “Test”, “Retest” and “Test”, or “Anesthesia-exposed” and “Retest”.

**2.1.3.2. Pharmacokinetic Modeling.** Using all data of a 60 min scan, the two-tissue compartment model (2TCM) showed lower Akaike values than the one-tissue compartment model (1TCM) for all brain regions. Based on the AIC, the 2TCM should be the model of choice for data analysis; however, the standard errors (SE%) of the estimated rate constants  $K_1$  and  $k_2$  were lower in the 1TCM than in the 2TCM. The large SE% of  $K_1$  and  $k_2$  in the 2TCM results in extremely high  $K_1$  and  $k_2$  values in all groups (more details in supplemental Table 2). Due to the insufficient stability of a 2TCM fit, the 1TCM was selected as the preferred kinetic model for  $[^{18}\text{F}]\text{MC225}$ .

Statistical analysis of the data of 1TCM fits did not find significant differences in the  $K_1$  values between the scans. However, the analysis found significant differences in the

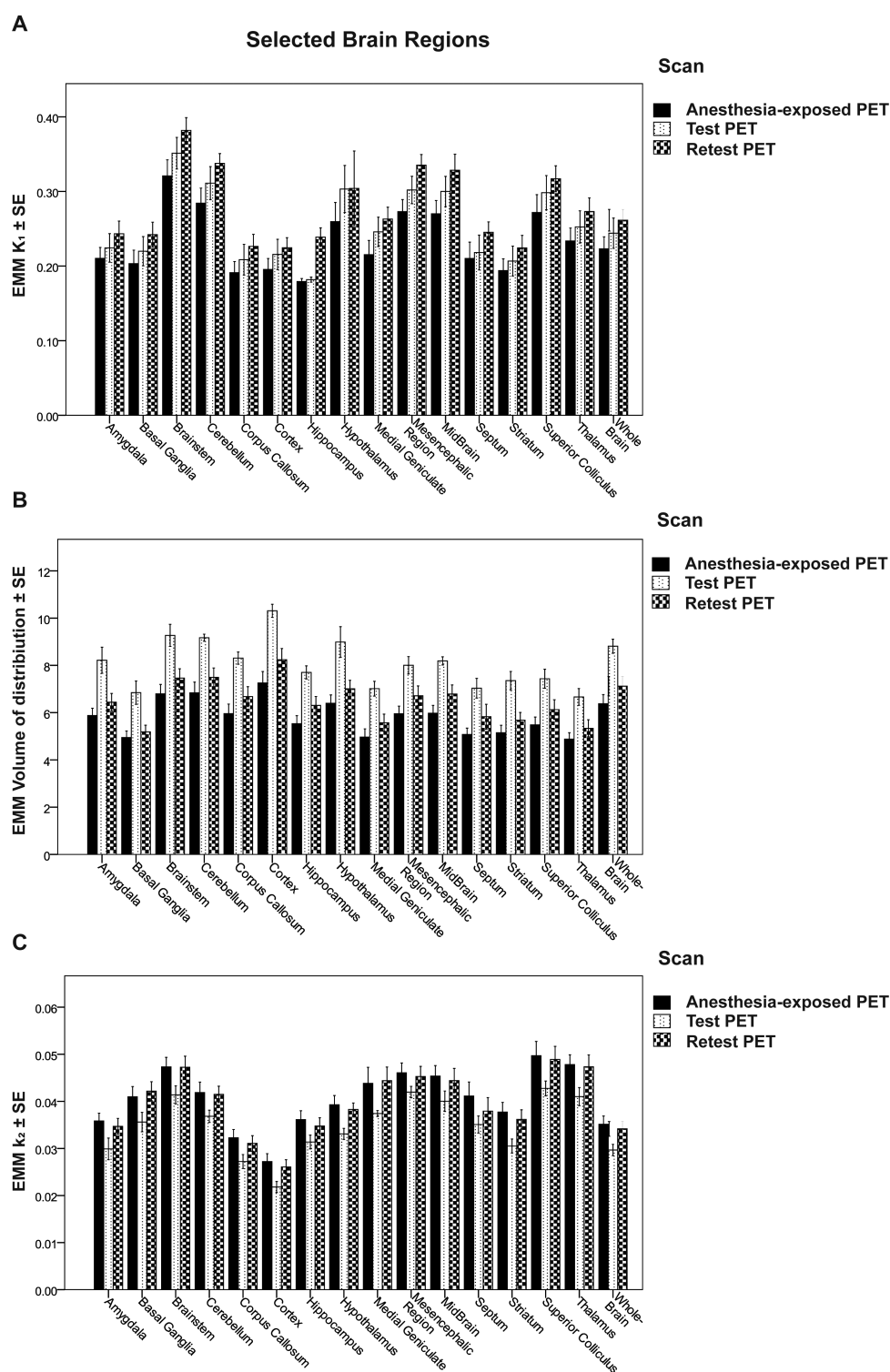


**Figure 5.** Regional  $K_1$  (A),  $V_T$  (B), and  $k_2$  (C) values of  $[^{18}\text{F}]\text{MC225}$  at different scans. Data expressed as  $\text{EMM} \pm \text{SE}$ .

whole-brain volume of distribution ( $V_T$ ) between the “Anesthesia-exposed” and “Test” scans ( $6.4 \pm 0.4$  vs  $8.8 \pm 0.3$ ;  $p < 0.001$ ) and also between “Retest” and “Test” ( $7.1 \pm 0.4$  vs  $8.8 \pm 0.3$ ;  $p < 0.001$ ) (Figure 3). Moreover, the analysis showed that the efflux constant  $k_2$  was significantly higher in the “Anesthesia-exposed” scans than in “Test” ( $0.035 \pm 0.002$  vs  $0.030 \pm 0.001$ ;  $p = 0.005$ ), and in “Retest” scans than in “Test” ( $0.034 \pm 0.001$  vs  $0.030 \pm 0.001$ ;  $p = 0.008$ ). No

significant differences in the  $V_T$ ,  $k_2$ , or  $K_1$  between the “Anesthesia-exposed” scan and “Retest” were found.

A rise of  $k_2$  may have caused a decrease of  $V_T$  in the “Anesthesia-exposed” and “Retest” scans (see Figures 3 and 4).

Similar significant group differences in  $V_T$  and  $k_2$  and a similar absence of significant differences in  $K_1$  were observed in the studied brain regions. Figure 5 shows the  $\text{EMM} \pm \text{SE}$  of  $K_1$ ,  $V_T$ , and  $k_2$  in the regions analyzed.

Table 1. EMM  $\pm$  SE  $V_T$ ,  $K_1$ , and  $k_2$  of the Selected Brain Region Using 30 min Scan Duration and 1TCM

region	Anesthesia-exposed PET			Test PET			Retest PET		
	mean $K_1 \pm$ SE	mean $k_2 \pm$ SE	mean $V_T \pm$ SE	mean $K_1 \pm$ SE	mean $k_2 \pm$ SE	mean $V_T \pm$ SE	mean $K_1 \pm$ SE	mean $k_2 \pm$ SE	mean $V_T \pm$ SE
amygdala	0.22 $\pm$ 0.01	0.047 $\pm$ 0	4.73 $\pm$ 0.24	0.25 $\pm$ 0.01	0.041 $\pm$ 0	6.13 $\pm$ 0.4	0.24 $\pm$ 0.02	0.045 $\pm$ 0	5.22 $\pm$ 0.24
basal ganglia	0.21 $\pm$ 0.02	0.05 $\pm$ 0	4.19 $\pm$ 0.22	0.24 $\pm$ 0.01	0.045 $\pm$ 0	5.55 $\pm$ 0.42	0.23 $\pm$ 0.02	0.053 $\pm$ 0	4.35 $\pm$ 0.22
brainstem	0.33 $\pm$ 0.02	0.057 $\pm$ 0	5.87 $\pm$ 0.32	0.38 $\pm$ 0.02	0.05 $\pm$ 0	7.69 $\pm$ 0.39	0.36 $\pm$ 0.02	0.056 $\pm$ 0	6.49 $\pm$ 0.3
cerebellum	0.3 $\pm$ 0.02	0.052 $\pm$ 0	5.74 $\pm$ 0.36	0.34 $\pm$ 0.01	0.047 $\pm$ 0	7.29 $\pm$ 0.32	0.32 $\pm$ 0.02	0.051 $\pm$ 0	6.33 $\pm$ 0.31
corpus callosum	0.2 $\pm$ 0.01	0.04 $\pm$ 0	5.06 $\pm$ 0.36	0.23 $\pm$ 0.01	0.035 $\pm$ 0	6.5 $\pm$ 0.33	0.22 $\pm$ 0.02	0.038 $\pm$ 0	5.66 $\pm$ 0.33
cortex	0.2 $\pm$ 0.01	0.034 $\pm$ 0	5.98 $\pm$ 0.4	0.23 $\pm$ 0.01	0.029 $\pm$ 0	7.9 $\pm$ 0.42	0.22 $\pm$ 0.02	0.033 $\pm$ 0	6.8 $\pm$ 0.37
hippocampus	0.21 $\pm$ 0.01	0.046 $\pm$ 0	4.53 $\pm$ 0.29	0.25 $\pm$ 0.01	0.041 $\pm$ 0	5.96 $\pm$ 0.31	0.23 $\pm$ 0.02	0.044 $\pm$ 0	5.19 $\pm$ 0.29
hypothalamus	0.26 $\pm$ 0.02	0.048 $\pm$ 0	5.44 $\pm$ 0.29	0.3 $\pm$ 0.02	0.042 $\pm$ 0	7.15 $\pm$ 0.46	0.28 $\pm$ 0.02	0.048 $\pm$ 0	5.88 $\pm$ 0.26
medial geniculate	0.22 $\pm$ 0.02	0.054 $\pm$ 0	4.26 $\pm$ 0.37	0.26 $\pm$ 0.01	0.045 $\pm$ 0	5.92 $\pm$ 0.4	0.26 $\pm$ 0.02	0.053 $\pm$ 0	4.82 $\pm$ 0.23
mesencephalic region	0.28 $\pm$ 0.01	0.055 $\pm$ 0	5.2 $\pm$ 0.28	0.34 $\pm$ 0.02	0.051 $\pm$ 0	6.65 $\pm$ 0.39	0.31 $\pm$ 0.02	0.054 $\pm$ 0	5.88 $\pm$ 0.35
midbrain	0.28 $\pm$ 0.02	0.055 $\pm$ 0	5.15 $\pm$ 0.3	0.33 $\pm$ 0.02	0.049 $\pm$ 0	6.77 $\pm$ 0.3	0.31 $\pm$ 0.02	0.053 $\pm$ 0	5.9 $\pm$ 0.35
septum	0.22 $\pm$ 0.02	0.052 $\pm$ 0	4.23 $\pm$ 0.24	0.25 $\pm$ 0.01	0.045 $\pm$ 0	5.57 $\pm$ 0.43	0.23 $\pm$ 0.02	0.048 $\pm$ 0	4.92 $\pm$ 0.47
striatum	0.2 $\pm$ 0.02	0.047 $\pm$ 0	4.35 $\pm$ 0.27	0.23 $\pm$ 0.01	0.038 $\pm$ 0	5.91 $\pm$ 0.39	0.22 $\pm$ 0.02	0.045 $\pm$ 0	4.77 $\pm$ 0.26
superior colliculus	0.28 $\pm$ 0.02	0.061 $\pm$ 0	4.69 $\pm$ 0.26	0.32 $\pm$ 0.02	0.054 $\pm$ 0	6.06 $\pm$ 0.41	0.31 $\pm$ 0.02	0.06 $\pm$ 0	5.21 $\pm$ 0.35
thalamus	0.24 $\pm$ 0.02	0.058 $\pm$ 0	4.17 $\pm$ 0.22	0.28 $\pm$ 0.01	0.052 $\pm$ 0	5.37 $\pm$ 0.34	0.26 $\pm$ 0.02	0.057 $\pm$ 0	4.64 $\pm$ 0.29
whole brain	0.23 $\pm$ 0.02	0.044 $\pm$ 0	5.3 $\pm$ 0.31	0.26 $\pm$ 0.01	0.038 $\pm$ 0	6.89 $\pm$ 0.36	0.25 $\pm$ 0.02	0.043 $\pm$ 0	5.93 $\pm$ 0.31

Table 2. Reliability of  $K_1$  Values between “Test” and “Retest” Scans in All the Brain Regions

regions	$K_1$ Test $\pm$ SD	$K_1$ Retest $\pm$ SD	Rel. Diff. $K_1$ (%)	TRV $K_1$ (%)	CV (%) $K_1$ test	CV (%) $K_1$ Retest	ICC $K_1$
amygdala	0.24 $\pm$ 0.04	0.21 $\pm$ 0.04	-7.75	8.07	15.61	20.88	0.287
cerebellum	0.34 $\pm$ 0.03	0.3 $\pm$ 0.04	-7.86	8.18	8.65	17.44	0.15
corpus callosum	0.23 $\pm$ 0.04	0.19 $\pm$ 0.03	-7.91	8.24	15.83	24.14	0.521
medial geniculate	0.26 $\pm$ 0.04 <sup>a</sup>	0.23 $\pm$ 0.03 <sup>a</sup>	-6.52	6.74	13.42	19.60	0.741
mesencephalic region	0.34 $\pm$ 0.03	0.29 $\pm$ 0.02	-9.95	10.47	9.48	14.89	-0.04
septum	0.25 $\pm$ 0.03 <sup>a</sup>	0.2 $\pm$ 0.03 <sup>a</sup>	-11.07	11.72	12.72	26.20	0.537
superior colliculus	0.32 $\pm$ 0.04	0.28 $\pm$ 0.04	-5.90	6.08	12.26	18.83	0.493
striatum	0.22 $\pm$ 0.04	0.19 $\pm$ 0.03	-7.89	8.22	16.70	23.79	0.616
cortex	0.22 $\pm$ 0.03	0.2 $\pm$ 0.04	-4.01	4.09	13.44	23.11	0.692
hippocampus	0.24 $\pm$ 0.03	0.21 $\pm$ 0.04	-8.86	9.28	14.34	22.80	0.555
hypothalamus	0.3 $\pm$ 0.04	0.26 $\pm$ 0.05	-8.94	9.35	13.96	19.04	0.688
mid brain	0.33 $\pm$ 0.05	0.28 $\pm$ 0.03	-8.67	9.06	14.66	16.59	0.128
brainstem	0.38 $\pm$ 0.04	0.34 $\pm$ 0.04	-7.98	8.31	10.01	14.78	-0.021
thalamus	0.27 $\pm$ 0.04	0.23 $\pm$ 0.03	-7.53	7.82	15.02	20.94	0.428
basal ganglia	0.24 $\pm$ 0.04	0.2 $\pm$ 0.03	-9.18	9.62	15.40	21.83	0.37
whole brain	0.26 $\pm$ 0.03	0.23 $\pm$ 0.04	-6.65	6.88	12.38	20.42	0.522
mean $\pm$ SD			-7.92 $\pm$ 1.66	8.26 $\pm$ 1.79	13.37 $\pm$ 2.36	20.33 $\pm$ 3.32	0.42 $\pm$ 0.25

<sup>a</sup>Significant differences between “Test” and “Retest” scan ( $p < 0.05$ ).

Several studies suggest that the best method to evaluate the P-gp function is to use the first part of the PET scan after the tracer injection.<sup>7,15</sup> At early time points, the metabolism of the tracer is still limited and therefore radiometabolites may not interfere with the P-gp measurement. For this reason, the kinetic analysis was also performed using a 30 min scan duration. Similar results to the 60 min scan analysis were obtained (see Table 1).

**2.1.4. Test–Retest Analysis.** The “Test” and “Retest” scans did not differ significantly regarding the injected dose ( $31 \pm 5.7$  MBq;  $p = 0.356$ ), the molar activity ( $58 \pm 21.7$  TBq;  $p = 0.868$ ) or the radiochemical purity ( $99.5 \pm 0.4\%$ ;  $p = 0.350$ ). Animals in “Retest” scans were 1 week older than during the “Test”, however, no significant differences in the body weight of animals between “Test” and “Retest” scans were found. (weight in “Test” scans =  $345 \pm 29$  vs weight in “Retest” =  $366 \pm 31$ ,  $p = 0.520$ ).

The  $K_1$  values were not significantly different between “Test” and “Retest” scans in any of the brain regions with the

exception of the medial geniculate region and septum (Table 2). Regarding the reproducibility evaluation, the relative difference (Rel. Diff. %) in  $K_1$  between “Test” and “Retest” scans varied from -4 to -11% and the absolute variability or Test–Retest variability (TRV%) was lower than 12% in all the regions. The coefficient of variance (CV%) in “Test” scans showed an average for all the brain regions of  $13 \pm 2\%$  and in “Retest” scans of  $20 \pm 3\%$ . Even though the average of the intraclass correlation coefficient (ICC) value for all the regions indicated a fair agreement between “Test” and “Retest” scans, most of the regions showed ICC values between 0.5 and 0.6, including the whole brain region, which indicated a moderate agreement.

In the case of the  $V_T$  values, the  $t$  test analysis found significant differences in all the brain regions between “Test” and “Retest” scans except for the septum (Table 3). The Rel. Diff. % values in  $V_T$  were larger than the ones from  $K_1$ , ranging between 16% and 24%, and TRV% was above 19% in all the brain regions. The between-subject repeatability expressed as

**Table 3. Reliability of the  $V_T$  Values between “Test” and “Retest” Scans in All the Brain Regions**

regions	$V_T$ Test $\pm$ SD	$V_T$ Retest $\pm$ SD	Rel. Diff. $V_T$ (%)	TRV $V_T$ (%)	CV (%) $V_T$ test	CV (%) $V_T$ Retest	ICC $V_T$
amygdala	8.22 $\pm$ 1.24 <sup>a</sup>	6.28 $\pm$ 0.91 <sup>a</sup>	-21.61	24.23	15.07	14.07	0.512
cerebellum	9.17 $\pm$ 0.33 <sup>a</sup>	7.42 $\pm$ 1.08 <sup>a</sup>	-18.29	20.13	3.62	14.42	0.236
corpus callosum	8.31 $\pm$ 0.58 <sup>a</sup>	6.49 $\pm$ 1.03 <sup>a</sup>	-19.63	21.76	6.97	15.49	0.225
medial geniculate	7.01 $\pm$ 0.7 <sup>a</sup>	5.49 $\pm$ 0.96 <sup>a</sup>	-20.52	22.86	9.95	17.28	0.372
mesencephalic region	8.01 $\pm$ 0.82 <sup>a</sup>	6.62 $\pm$ 1.11 <sup>a</sup>	-16.13	17.55	10.19	16.58	0.533
septum	7.04 $\pm$ 0.93	5.59 $\pm$ 1.29	-17.18	18.79	13.25	22.08	0.317
superior colliculus	7.44 $\pm$ 0.9 <sup>a</sup>	6.05 $\pm$ 1.12 <sup>a</sup>	-17.55	19.24	12.12	18.23	0.575
striatum	7.35 $\pm$ 0.87 <sup>a</sup>	5.55 $\pm$ 0.82 <sup>a</sup>	-22.75	25.67	11.86	14.45	0.354
cortex	10.31 $\pm$ 0.62 <sup>a</sup>	8.12 $\pm$ 1.25 <sup>a</sup>	-20.09	22.34	5.97	15.23	0.259
hippocampus	7.7 $\pm$ 0.62 <sup>a</sup>	6.14 $\pm$ 0.93 <sup>a</sup>	-18.16	19.97	8.07	14.76	0.338
hypothalamus	8.99 $\pm$ 1.45 <sup>a</sup>	6.92 $\pm$ 0.95 <sup>a</sup>	-22.00	24.73	16.13	13.56	0.494
mid brain	8.19 $\pm$ 0.39 <sup>a</sup>	6.77 $\pm$ 1.06 <sup>a</sup>	-17.14	18.75	4.76	15.65	0.313
brainstem	9.27 $\pm$ 1.04 <sup>a</sup>	7.45 $\pm$ 1.09 <sup>a</sup>	-19.50	21.61	11.26	14.61	0.57
thalamus	6.66 $\pm$ 0.79 <sup>a</sup>	5.22 $\pm$ 0.94 <sup>a</sup>	-19.90	22.10	11.86	17.56	0.506
basal ganglia	6.85 $\pm$ 1.11 <sup>a</sup>	5.06 $\pm$ 0.69 <sup>a</sup>	-24.23	27.57	16.15	13.33	0.434
whole brain	8.81 $\pm$ 0.67 <sup>a</sup>	7 $\pm$ 1.07 <sup>a</sup>	-19.18	21.22	7.58	15.01	0.373
mean $\pm$ SD			-19.62 $\pm$ 2.23	21.78 $\pm$ 2.75	10.3 $\pm$ 3.89	15.77 $\pm$ 2.2	0.4 $\pm$ 0.12

<sup>a</sup>Significant differences between Test and Retest scan ( $p < 0.05$ )

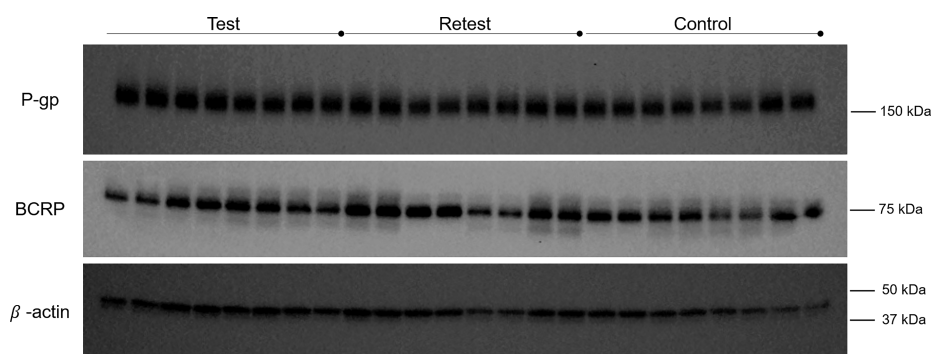


**Figure 6.** Western Blot bands corresponding to P-gp, BCRP, and  $\beta$ -actin (160, 72, and 42 kDa predicted molecular weight, respectively).

CV% showed an average for all the regions of  $10 \pm 4\%$  in “Test” scans and  $16 \pm 2\%$  in “Retest” scans. Most of the ICC values for the  $V_T$  varied from 0.2 to 0.3 which indicated slight agreement between “Test” and “Retest” scans.

**2.1.5. Blood Flow Analysis.** The statistical analysis did not reveal any significant difference in whole-brain SUV values of the first frames among the three study scans (SUV “Anesthesia-exposed” =  $0.85 \pm 0.049$  vs SUV “Test” =  $0.84 \pm 0.052$ ;  $p = 0.876$  and SUV “Retest” =  $0.91 \pm 0.025$  vs SUV “Test” =  $0.84 \pm 0.052$ ;  $p = 0.276$ ). This result indicates that anesthesia does not cause long-term alterations of cerebral blood flow (CBF).

**2.1.6. Western Blot.** Wistar rats with similar weights to the ones used during the PET scans were used for the WB analysis. These animals underwent the same procedures as the animals used in the PET studies: Group “Test” was once previously anesthetized, Group “Retest” was twice previously anesthetized, and the group control was not subjected to anesthesia before the euthanasia. WB analysis showed no significant differences in P-gp and BCRP expression between the control group and any of the anesthetized groups (“Test” and “Retest” groups) (see Figures 6 and 7).

**2.2. Discussion.** The plasma concentration of [ $^{18}\text{F}$ ]MC225 (corrected for metabolites) was significantly higher in the scans where the animals were pre-exposed to anesthesia, “Anesthesia-exposed” (+25%) and “Retest” (+19%). Moreover, the parent

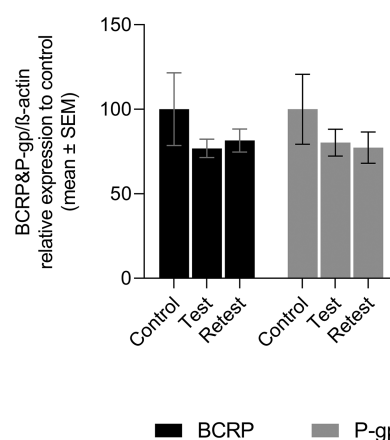


**Figure 7.** BCRP and P-gp expression in control animals, group “Test” (one time anesthetized) and group “Retest” (twice anesthetized). Expression was related to  $\beta$ -actin and then normalized to protein expression found in control animals. Data are shown as mean  $\pm$  SE ( $n$  per group = 4 with duplicates).

fraction of plasma radioactivity was slightly but significantly increased by 6% in “Anesthesia-exposed” animals and by 5% in “Retest”, both compared to “Test”. However, we did not observe significant differences in  $T_{1/2}$  among the scans. These results suggest that previous exposure to anesthesia may affect

the tracer concentration in plasma but not its rate of elimination.

Previous PET studies in rodents have identified 1TCM as the preferred model to analyze [ $^{18}\text{F}$ ]MC225 kinetics.<sup>10</sup> In our own study, 1TCM was also chosen as the best model to fit the data. The model fit indicates a significant decrease in the  $V_T$  of [ $^{18}\text{F}$ ]MC225 in whole-brain and all analyzed brain regions of animals pre-exposed to isoflurane-anesthesia (“Anesthesia-exposed” and “Retest”). We also observed a significant increase in  $k_2$  values of the tracer in whole-brain and in most brain regions analyzed. Whole-brain  $V_T$  was 28% lower in “Anesthesia-exposed” and 19% lower in “Retest” than in “Test” scans. Meanwhile, whole-brain  $k_2$  was 18% and 15% higher in “Anesthesia-exposed” and “Retest” scans compared to “Test”. On the other hand, tracer levels in the blood were higher in animals pre-exposed to anesthesia (“Anesthesia-exposed” and “Retest” scans) than in “Test”. However, the whole-brain SUV-TACs in the three scans were not significantly different. These changes may be related, i.e. the decrease in  $V_T$  due to previous exposure to anesthesia may be caused by the increase in  $k_2$ , resulting in reduced brain uptake and increased concentration of the radiotracer in plasma. However, the 1TCM fit did not indicate significant changes in the  $K_1$ , which is considered by many authors as the best parameter to measure the P-gp function at the BBB.<sup>7,8,10,15–17</sup>

Previous validation of [ $^{18}\text{F}$ ]MC225 as a tracer for measuring P-gp function at the BBB of rats found a significant increase in the  $K_1$  and  $V_T$  after the administration of the P-gp inhibitor tariquidar. This analysis also indicated that  $K_1$  values were stable during the whole PET scan, whereas the  $V_T$  values became stable only after 30 min scan duration. Furthermore, after P-gp inhibition, the observed changes in  $K_1$  were larger than the changes in  $V_T$ . Therefore, this study concluded that  $K_1$  is the best parameter to measure the P-gp function, although  $V_T$  may also be used when sufficient scan data (>30 min) are available.<sup>10</sup>

In contrast to these findings, the pharmacokinetic evaluation of [ $^{11}\text{C}$ ]metoclopramide, another tracer considered as a weak P-gp substrate, indicated a significant decrease in the efflux constant  $k_2$  values after the administration of tariquidar which caused a significant increase of the brain  $V_T$  in rats and nonhuman primates.<sup>18,19</sup> The authors of these studies suggest the use of  $k_2$  as the best parameter to measure the P-gp function. Nevertheless, it has been discussed that  $V_T$  and  $k_2$  parameters can be affected by nonspecific trapping of the tracer and can also be affected by the fraction of radiometabolites inside the brain.<sup>7,15</sup>

One strategy to avoid the interference of radiometabolites in the kinetic evaluation is to use short scan duration, such as 30 min scans. For instance, Muzi et al. suggested the use of  $K_1$  calculated with 1TCM and a 30 min scan to evaluate the P-gp function at the human BBB using [ $^{11}\text{C}$ ]verapamil.<sup>7</sup> Following these suggestions, the kinetics of [ $^{18}\text{F}$ ]MC225 were also evaluated using 30 min of scan data. The same results were obtained for 30 and 60 min scans. The kinetic parameters such as  $V_T$ ,  $K_1$ , and  $k_2$  were calculated using 1TCM which was selected as the preferred model. No significant changes in the  $K_1$  were observed, and the same significant decrease in the  $V_T$  and increase in  $k_2$  were found in data of short scans.

All these results combined could suggest that isoflurane anesthesia induces or activates the P-gp function at the BBB. However, the absence of significant changes in  $K_1$  refutes this hypothesis. Moreover, post-mortem analysis of brain tissue

with WB did not indicate any significant change in P-gp or BCRP expression in animals pre-exposed to anesthesia. Thus, isoflurane anesthesia does not increase the expression of P-gp at the BBB.

Taken together, our results confirm that  $K_1$  is indeed the best parameter to measure P-gp function at the BBB, since the lack of significant changes in  $K_1$  in animals exposed to anesthesia corresponds to the absence of significant changes in P-gp expression shown by WB. Moreover, this study suggests that values of  $V_T$  and  $k_2$  should be used with caution, since these values may change in longitudinal studies for unknown reasons.

The observed changes in  $V_T$  are in accordance with recent studies indicating that anesthesia may cause changes in the distribution or binding affinity of PET tracers.<sup>20</sup> For example, the use of chloral hydrate and ketamine markedly increases, and pentobarbital decreases, the binding potential of [ $^{11}\text{C}$ ]SCH23390 to dopamine  $D_1$  receptors compared to that in conscious rats.<sup>12</sup> Ketamine/xylazine also increases the binding potential of [ $^{11}\text{C}$ ]MNPA to  $D_2$  receptors compared to the binding in conscious animals.<sup>21</sup> Chronic diazepam treatment reduces the global uptake of [ $^{18}\text{F}$ ]FDG in the rat brain.<sup>22</sup> Moreover, isoflurane anesthesia seems to affect the sensitivity of agonist tracers for dopamine  $D_2$  receptors in an amphetamine challenge,<sup>23</sup> and to alter the metabolism of the P-gp tracer [ $^{11}\text{C}$ ]-*N*-desmethyl-loperamide.<sup>3</sup> Furthermore, a prolonged effect of sevoflurane has been observed on the kinetics of [ $^{11}\text{C}$ ]raclopride in nonhuman primates.<sup>24</sup>

These changes can also be explained by changes in CBF.<sup>20</sup> General anesthetics are known to affect CBF, e.g., propofol causing a decrease, whereas ketamine, isoflurane, sevoflurane and halothane cause a slight increase or do not affect global CBF.<sup>20,25–27</sup> Since isoflurane is expected to increase CBF,<sup>28,29</sup> the brain uptake of [ $^{18}\text{F}$ ]MC225 should have increased in animals pre-exposed to anesthesia. However, we did not observe any increase but rather a significant decrease in  $V_T$ . Moreover, whole-brain SUV of the tracer in the initial frames and the  $K_1$  values were not significantly different in the three study groups, suggesting that CBF was not significantly affected by previous exposure to anesthesia.

$V_T$  values at “Test” and “Retest” were significantly different in most of the regions analyzed, whereas  $K_1$  values were not. The  $K_1$  values showed an overall TRV% lower than 10%; however, in the case of  $V_T$ , TRV% was around 20%. ICC values indicated a moderate agreement between Test- Retest  $K_1$  values and only slight agreement for the  $V_T$  values. These results suggest that  $K_1$  values show better reproducibility and reliability than  $V_T$ . Therefore, in longitudinal studies aimed to assess the P-gp function under different conditions,  $K_1$  should be used.

The present study found a significant increase in  $k_2$  values which led to a significant decrease of  $V_T$  values of [ $^{18}\text{F}$ ]MC225 inside the brain of animals pre-exposed to anesthesia. However, the study did not find significant changes in the  $K_1$ , which is considered as the best parameter to measure the P-gp function. These results were supported by the WB experiment which did not find any significant increase in the P-gp or BCRP expression of animals pre-exposed to anesthesia. Overall, our results suggest that isoflurane-anesthesia affects the brain distribution of [ $^{18}\text{F}$ ]MC225 causing changes in  $V_T$  and  $k_2$ ; however, anesthesia does not alter P-gp expression at the BBB. Longitudinal studies with [ $^{18}\text{F}$ ]MC225 are possible if  $K_1$  is used to estimate the function of P-gp.

### 3. METHODS

**3.1. Chemicals.** The precursor of [ $^{18}\text{F}$ ]MC225, 5-[3-(6,7-dimethoxy-3,4-dihydro-1H-isoquinolin-2-yl)-propyl]-5,6,7,8-tetrahydro-naphthalen-1-ol (MC226), was purchased from Syncom (Groningen, The Netherlands). Chemicals were purchased from Sigma-Aldrich (St. Louis, MO), and isoflurane was purchased from Pharmachemie (Haarlem, The Netherlands).

**3.2. Tracer Production.** [ $^{18}\text{F}$ ]MC225 was synthesized as previously described.<sup>9</sup>

**3.3. Animals.** Thirteen healthy male Wistar rats were purchased from Janvier Laboratories (France). Before the start of the experiments, rats were acclimatized for at least 7 days. Rats were housed individually after the first procedure. The room was kept at a constant temperature ( $21 \pm 2^\circ\text{C}$ ) with a 12/12 h light/dark regimen. The rats were fed ad libitum, and water was always available. Rat weight ( $354 \pm 38\text{ g}$ ) and behavior were monitored throughout the entire study. All applicable institutional and/or national guidelines for the care and use of animals were followed. The experiments were performed in compliance with Dutch and EU regulations. The protocol was approved by the National Committee on Animal Experiments of The Netherlands (CCD, the Hague) and the Institutional Animal Care and Use Committee of the University of Groningen (CCD license number: AVD105002015166, IvD protocol 15166-01-002).

Moreover, 17 Wistar rats (Janvier Laboratories, France) were used for WB studies. Rats were acclimatized for at least 7 days and were housed in groups (3 rats per cage). The rats were kept under controlled environment conditions (constant temperature of  $22 \pm 1^\circ\text{C}$  and 12 h light/12 h dark cycle and  $60 \pm 5\%$  humidity). Food and water were allowed ad libitum. The weight ( $354 \pm 26\text{ g}$ ), and the behavior of the rats was monitored during the study. The experimental protocol was approved by the local Animal Care Committee according to the European Union (EU) rules (86/609/CEE, 2003/65/CE, and 2010/63/EU).

**3.4. Study Design.** Regarding the PET studies, rats were divided into two groups. Group 1 was used to evaluate the effect of the anesthesia on the P-gp transporters and group 2 was used to assess the reproducibility of [ $^{18}\text{F}$ ]MC225 data, with an interval of 1 week between the scans. On day 7, after arrival and acclimatization, group 1 animals ( $n = 7$ ) were transported to the PET facility and anesthetized with isoflurane in oxygen (5% for induction, 1.5–2% for maintenance, during  $72 \pm 17\text{ min}$ ), whereas group 2 animals ( $n = 6$ ) were transported but not subjected to anesthesia. On day 14, a dynamic PET scan with arterial blood sampling (60 min) was made for all rats. The scan of group 1 (made after previous exposure to anesthesia) was referred to as “Anesthesia-exposed”, and the first scan of group 2 was indicated as “Test” (these animals had not been previously exposed to anesthesia). On day 21, a second dynamic PET scan was made for the rats of group 2. This scan is referred to as “Retest” (study design details in Figure 8). All PET scans were performed under isoflurane anesthesia. Thus, “Retest” animals had been previously exposed to anesthesia, during their “Test” scan. Therefore, in “Anesthesia-exposed” and “Retest” PETs, the animals were anesthetized twice, and in the “Test” animals were anesthetized only once. Before each scan, a

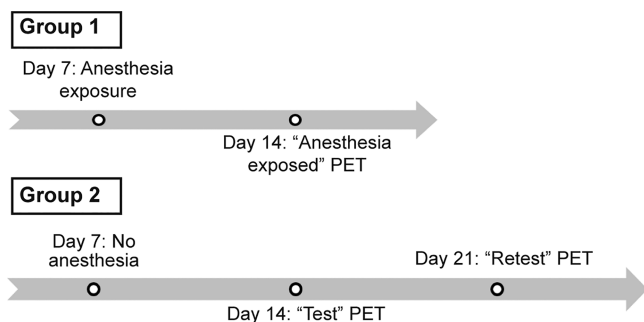


**Figure 8.** PET study design: group 1 (above) and group 2 (below).

cannula was placed in a side branch of the femoral artery for blood sampling during the scan.<sup>30</sup> During this surgery, the rats were also under anesthesia for about 30 min. Anesthesia for surgery and PET scanning lasted 86–120 min. It is important to note that, at the “Retest” scan, animals of group 2 had also been subjected twice to surgery (cannula placement), which may have induced extra stress. The body temperature of anesthetized animals was maintained close to the normal value with heating pads and electronic temperature controllers. Blood oxygenation and heart rate were continuously monitored during the scan, using pulse oximeters.

Rats from WB studies were divided into three groups (Figure 9). The “Test” group ( $n = 6$ ) was exposed to isoflurane anesthesia only once, on day 14. The “Retest” group ( $n = 6$ ) was exposed twice to anesthesia, on days 7 and 14; and the control group ( $n = 5$ ) was not previously exposed to anesthesia. The anesthesia exposure consisted of  $6 \pm 1\text{ min}$  for induction (4%, 2.1 L/min) and  $89 \pm 5\text{ min}$  for maintenance (2%, 1.5 L/min). During maintenance, rats were anesthetized with a mask and the body temperature was controlled and kept close to normal values with a heating pad. On day 14, all rats were terminated by decapitation under deep anesthesia after phosphate buffered saline (PBS) perfusion and brains were immediately collected. The brain tissue was flash-frozen in liquid nitrogen and stored at  $-80^\circ\text{C}$  until samples were analyzed.

**3.5. PET Data Collection.** Anesthetized rats were placed in the PET camera (Focus 220; Siemens Medical Solution Inc.). The head of the rats was placed in the field of view.

First, a transmission scan was made using a  $^{57}\text{Co}$  point source for attenuation and scatter correction. Rats were then injected with [ $^{18}\text{F}$ ]MC225 via a tail vein ( $32.5 \pm 5.5\text{ MBq}$ , in 1 mL during 1 min, using a Harvard infusion pump), and the dynamic emission scan of 60 min was started simultaneously.

PET images were normalized and corrected for attenuation and decay. Emission sinograms were iteratively reconstructed using OSEM 2D, 4 iterations, and 16 subsets. The list-mode data of the emission scan was reconstructed into 21 frames ( $6 \times 10$ ;  $4 \times 30$ ;  $2 \times 60$ ;  $1 \times 120$ ;  $1 \times 180$ ;  $4 \times 300$ ;  $3 \times 600\text{ s}$ ).

**3.6. Blood Data Collection.** During the scan, blood samples (0.1–0.15 mL) were drawn from the arterial cannula at 10, 20, 30, 40, 50, and 60 s and 1, 1.5, 2, 3, 5, 7.5, 10, 15, 30, and 60 min after tracer injection. The total volume drawn was less than 2 mL. A 25  $\mu\text{L}$  sample of whole-blood was used for radioactivity measurements. The remaining volume of the samples was centrifuged at 6000 rpm (Mikro 20, Hettich, Germany) for 5 min to separate blood and plasma. A volume of 25  $\mu\text{L}$  of plasma was taken for radioactivity measurements and placed on ice to limit tracer metabolism. The radioactivity in blood and plasma was measured with a  $\gamma$ -counter (LKB Wallac, Turku, Finland), and values were corrected for decay.

The fractions of the parent [ $^{18}\text{F}$ ]MC225 and of radioactive metabolites were determined using thin-layer chromatography (TLC) analysis. Plasma proteins were precipitated by the addition of acetonitrile (50  $\mu\text{L}$ ) to the plasma samples. After measurement of radioactivity in the  $\gamma$ -counter, plasma samples were mixed by vortexing for less than 1 min and were centrifuged for 5 min at 6000 rpm (Hettich Mikro 20, Hettich Zentrifugen, Germany) to obtain a protein-free supernatant. A 2.5  $\mu\text{L}$  sample of each supernatant was spotted on a silica gel TLC plate. The TLC plate was eluted with 10% MeOH in EtOAc and was placed on an activated phosphor storage plate overnight. The storage plates were read using a Cyclone system (PerkinElmer Life and Analytical Science, Waltham, MA). OptiQuant 03.00 software (PerkinElmer) was used to calculate the fractions of parent tracer ( $R_f = 0.8\text{--}0.9$ ) and radioactive metabolites ( $R_f = 0.2$ ).

**3.7. Input Function Analysis.** Measured radioactivity in blood samples was corrected for decay from the time of tracer administration. The time–activity curves (TAC) of whole-blood, plasma, and metabolite-corrected plasma were expressed as standardized uptake value (SUV):  $\text{SUV} = \text{radioactive concentration (MBq/ml)} / [\text{injected dose (MBq)} / \text{body weight (g)}]$ . The metabolite-corrected plasma TAC-SUV was obtained by multiplying the SUV values of the plasma samples by the parent fraction.

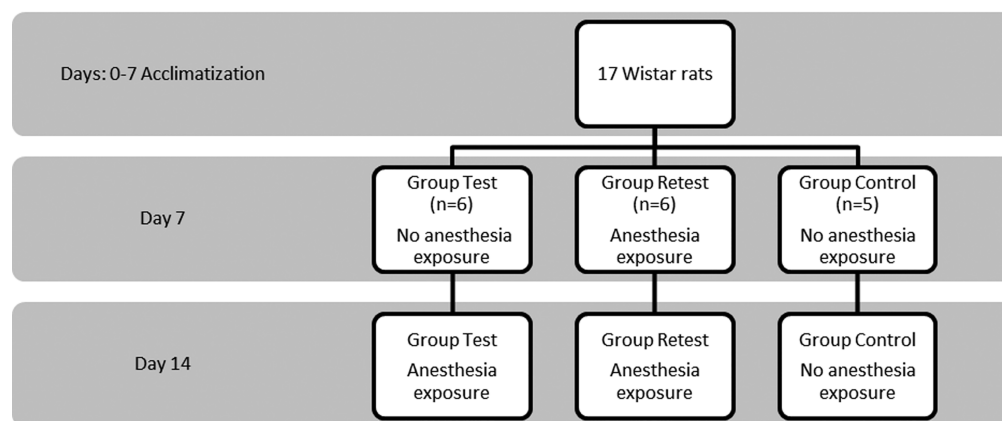


Figure 9. Western Blot study design.

A single exponential curve was fitted to the TAC-SUV of metabolite-corrected plasma (using values from 62 to 3564 s) by iterative nonlinear least-squares approach using GraphPad software (GraphPad Prism version 7.02, San Diego, CA) to calculate the biological half-life of the tracer ( $T_{1/2}$ ):  $Y = Y_0 \exp(-K_e X)$ , where  $Y$  is the metabolite-corrected SUV value in plasma,  $Y_0$  is the  $Y$ -intercept,  $K_e$  is the first-order rate constant of elimination, and  $X$  is the time. Tracer biological half-life was calculated as  $T_{1/2} = \ln(2)/K_e$ .<sup>31</sup>

**3.8. PET Image Processing.** All PET images were automatically registered by rigid transformation to a [<sup>18</sup>F]MC225 specific template, which was spatially aligned to a T2-weighted MRI of a Wistar rat in Paxinos space.<sup>32</sup> Images were processed using PMOD v3.8 software (PMOD Technologies, Zürich, Switzerland).

Sixteen volumes of interest (VOI) were selected from a rat brain atlas:<sup>32</sup> amygdala, cerebellum, corpus callosum, medial geniculate, mesencephalic, septum, superior colliculus, striatum, cortex, hippocampus, hypothalamus, midbrain, brainstem, thalamus, basal ganglia, and whole brain. The radioactivity concentration was calculated for each selected brain region to generate TACs, and it was expressed as SUV.

**3.9. Pharmacokinetic Modeling.** The TACs of whole-blood and plasma corrected for metabolites were used for pharmacokinetic modeling using PMOD v3.8. In this study, 1TCM and 2TCM were evaluated using 30 and 60 min scan duration. The most appropriate model was selected based on the Akaike Information Criterion (AIC) which measures the goodness of the fit. The standard errors (SE%) of the estimated parameters were also taken into account during the model selection. The cerebral blood volume fraction was fixed to 5% following the recommendation from a previous preclinical study.<sup>10</sup> The most appropriate model was used to calculate the influx ( $K_1$ ) and efflux ( $k_2$ ) rate constants and the volume of distribution ( $V_T$ ).

**3.10. Test–Retest Analysis.** The reproducibility of [<sup>18</sup>F]MC225 scans was evaluated using the Rel. Diff. % between “Test” and “Retest” scans, TRV% between both measurements and the between-subject standard deviation was evaluated with the CV% for “Test” and “Retest” measurements. All these parameters were calculated according to methods of Elmenhorst et al.<sup>33</sup>

Relative Differences (Rel. Diff%)

$$= [(Retest - Test)/Test] \times 100$$

Test – Retest Variability (TRV%)

$$= [(Retest - Test)/((Retest + Test)/2)] \times 100$$

Coefficient of Variance (CV%) = (SD/mean)  $\times$  100

The reliability of the measurements between and within subject was evaluated using the ICC. This analysis was performed using a 2-way mixed model with absolute agreement type and a confidence interval of 95%. IBM SPSS Statistics version 23 (Armonk, NY) was used. ICC values between 0 and 0.2, 0.3 and 0.4, 0.5 and 0.6, 0.7 and 0.8, and 0.9

and 1 are categorized as slight, fair, moderate, substantial and almost perfect agreement, respectively.<sup>30,34</sup>

**3.11. Blood Flow Analysis.** In the case of tracers with high extraction fraction, the early frames of a dynamic PET scan provide information about tracer delivery and, thus, about blood flow changes.<sup>35</sup> Since [<sup>18</sup>F]MC225 has a log  $D$  of 3, it is considered as a lipophilic tracer with a high extraction fraction.<sup>9</sup> Hence, in order to assess changes in blood flow after a previous exposure of animals to anesthesia, SUV values for whole-brain were calculated from frame 3 to 12 (from 20 to 300 s).

**3.12. Western Blot Analysis.** P-gp and BCRP expression were quantified by means of WB. Protein extraction was carried out adding cold RIPA buffer (Sigma, USA) with protease inhibitor cocktail (Sigma, USA) to brain slices in an approximated 10:1 proportion (volume/weight) and tissue disruption was performed in a TissueLyser II instrument (Qiagen, Switzerland). Then tissue lysates were centrifuged for 30 min at 20 000g, and supernatants were collected to perform WB. Protein concentration in the lysates was quantified using the Micro BCA Protein assay kit (ThermoFisher, USA).

The necessary volume of cell lysate containing a total amount of 50  $\mu$ g of protein was subjected to SDS-PAGE in 4–15% Criterion TGX Precast Midi Protein Gel (BioRad, USA) using a constant voltage of 140 V. Then proteins were transferred onto a PVDF membrane (Millipore, Ireland) using a Trans-Blot semidry system (Bio-Rad, USA) with a limited voltage of 25 V and 180 milliamps for two hours.

After the blotting step, membranes were blocked for 1 h with a 3% bovine serum albumin (BSA) solution (in Tris-chloride buffer with 0.1% Tween 20 (TBST)). Once blocked, target proteins were detected through the incubation with primary antibodies against P-gp (rabbit monoclonal to P glycoprotein ab170904, Abcam, UK), BCRP (rabbit polyclonal to BCRP/ABCG2 ab63907, Abcam, UK), and  $\beta$ -actin (mouse monoclonal to  $\beta$ -Actin ab8226, Abcam, UK) diluted to 1:1000, 1:1000, and 1:5000, respectively, in TBST with 3% BSA. Primary antibodies were incubated overnight at room temperature under agitation, and then membranes were washed three times in TBST in order to remove the excess of primary antibodies and avoid unspecific signaling. As secondary antibodies, HRP-conjugated goat anti-rabbit IgG (P044801-2, Dako, Denmark) and HRP-conjugated rabbit anti-mouse IgG (P026002-2, Dako, Denmark) were used. They were diluted to 1:5000 in TBST with 3% BSA and incubated for 1 h at room temperature under agitation. Eventually, after washing, the HRP activity was revealed with Pierce ECL Western Blotting Substrate (Thermo Fisher, USA) and detected in a Chemi Doc MP imaging system (BioRad, USA).

WB results were analyzed measuring the mean gray value of protein bands delimited in regions of interest using ImageJ software. The relative expression of P-gp and BCRP to  $\beta$ -actin was calculated for each sample, and the average of samples for each group was normalized to the control.

**3.13. Statistical Analysis.** Results are presented as mean  $\pm$  SE or EMM  $\pm$  SE unless otherwise indicated. IBM SPSS Statistics version 23 was used for statistical analysis. Group differences in  $V_T$ ,  $K_1$ ,  $k_2$ , SUV-TACs, and  $T_{1/2}$  were assessed by generalized estimated equation (GEE) with the independent matrix.<sup>36</sup> Results were considered statistically significant at  $p < 0.05$ , without correction for multiple comparisons. The variability of  $V_T$  and the rate constant  $k_2$  between “Test” and “Retest” (or “Test” and “Anesthesia-exposed”) was calculated using the “Test” scan as the reference, using the formulas:  $(V_T(k_2) \text{ “Anesthesia-exposed”} - V_T(k_2) \text{ “Test”})/V_T(k_2) \text{ “Test”}$  and  $(V_T(k_2) \text{ “Retest”} - V_T(k_2) \text{ “Test”})/V_T(k_2) \text{ “Test”}$ . Both values are expressed as percentages. Differences in injected dose, molar activity, radiochemical purity, and body weight between “Test” and “Retest” scans (Group 2) were evaluated using paired  $t$  test, and  $p$  values  $< 0.05$  were considered statistically significant.

## ■ ASSOCIATED CONTENT

### SI Supporting Information

The Supporting Information is available free of charge at <https://pubs.acs.org/doi/10.1021/acchemneuro.9b00682>.

Table with values of tracer concentration in plasma, whole-blood and plasma-corrected for metabolites and the parent fraction in different groups; statistical significance of differences between scans; table with Akaike values, SE% $K_1$  and SE% $k_2$  for 1TCM and 2TCM fits using 60 min scan duration (PDF)

## ■ AUTHOR INFORMATION

### Corresponding Author

**Gert Luurtsema** – Department of Nuclear Medicine and Molecular Imaging, University of Groningen, University Medical Center Groningen, 9713 GZ Groningen, The Netherlands; Email: [g.luurtsema@umcg.nl](mailto:g.luurtsema@umcg.nl)

### Authors

**Lara García-Varela** – Department of Nuclear Medicine and Molecular Imaging, University of Groningen, University Medical Center Groningen, 9713 GZ Groningen, The Netherlands;

[orcid.org/0000-0001-9803-4708](https://orcid.org/0000-0001-9803-4708)

**David Váñez García** – Department of Nuclear Medicine and Molecular Imaging, University of Groningen, University Medical Center Groningen, 9713 GZ Groningen, The Netherlands

**Manuel Rodríguez-Pérez** – Clinical Neurosciences Research Laboratory, Health Research Institute of Santiago de Compostela (IDIS), Santiago de Compostela 15706, Spain

**Aren van Waarde** – Department of Nuclear Medicine and Molecular Imaging, University of Groningen, University Medical Center Groningen, 9713 GZ Groningen, The Netherlands

**Jürgen W. A. Sijbesma** – Department of Nuclear Medicine and Molecular Imaging, University of Groningen, University Medical Center Groningen, 9713 GZ Groningen, The Netherlands

**Anna Schildt** – Department of Nuclear Medicine and Molecular Imaging, University of Groningen, University Medical Center Groningen, 9713 GZ Groningen, The Netherlands

**Chantal Kwizera** – Department of Nuclear Medicine and Molecular Imaging, University of Groningen, University Medical Center Groningen, 9713 GZ Groningen, The Netherlands

**Pablo Aguiar** – Department of Nuclear Medicine and Molecular Imaging Group, Clinical University Hospital, IDIS Health Research Institute, Santiago de Compostela 15706, Spain

**Tomás Sobrino** – Clinical Neurosciences Research Laboratory, Health Research Institute of Santiago de Compostela (IDIS), Santiago de Compostela 15706, Spain

**Rudi A. J. O. Dierckx** – Department of Nuclear Medicine and Molecular Imaging, University of Groningen, University Medical Center Groningen, 9713 GZ Groningen, The Netherlands

**Philip H. Elsinga** – Department of Nuclear Medicine and Molecular Imaging, University of Groningen, University Medical Center Groningen, 9713 GZ Groningen, The Netherlands

Complete contact information is available at:

<https://pubs.acs.org/doi/10.1021/acchemneuro.9b00682>

### Author Contributions

L.G.-V. contributed to the design of the study, performed the synthesis of the tracer, conducted the preclinical studies, did the kinetic analysis, and wrote the manuscript with help from all authors. D.V.G. contributed to the data analysis and to the preparation of the manuscript. M.R.-P. performed Western Blot studies. A.v.W. contributed to the design of the experiment, provided assistance during the in vivo studies (PET and analysis of blood samples), and commented on the final manuscript. J.W.A.S. and A.S. provided assistance during the in vivo studies. C.K. helped in the synthesis of the tracer. P.A. and T.S. helped in the design of the Western Blot studies and commented on the final manuscript. R.A.J.O.D. and P.H.E. commented on the final manuscript. G.L. contributed to the design of the experiment and helped in the interpretation of the data and in the preparation of the manuscript.

### Funding

P.A. (RYC-2015/17430) is a recipient of the Ramón y Cajal contract, T.S. (CPII17/00027) is a recipient of a research contract from the Miguel Servet Program (National Institute of Health Carlos III), and M.R.-P. is a recipient of a Xunta de Galicia fellowship PhD program (IN606A-2018/031).

### Notes

The funders had no role in the study design, data collection and analysis, decision to publish, or preparation of the manuscript.

The authors declare no competing financial interest.

## ■ REFERENCES

- (1) Gameiro, M., Silva, R., Rocha-Pereira, C., Carmo, H., Carvalho, F., Bastos, M. D. L., and Remião, F. (2017) Cellular Models and In Vitro Assays for the Screening of Modulators of P-Gp, MRP1 and BCRP. *Molecules* 22 (4), 600.
- (2) Miller, D. S., Bauer, B., and Hartz, A. M. S. (2008) Modulation of P-Glycoprotein at the Blood-Brain Barrier: Opportunities to Improve Central Nervous System Pharmacotherapy. *Pharmacol. Rev.* 60 (2), 196–209.
- (3) Wanek, T., Römermann, K., Mairinger, S., Stanek, J., Sauberer, M., Filip, T., Traxl, A., Kuntner, C., Pahnke, J., Bauer, F., Erker, T., Löscher, W., Müller, M., and Langer, O. (2015) Factors Governing P-Glycoprotein-Mediated Drug-Drug Interactions at the Blood-Brain Barrier Measured with Positron Emission Tomography. *Mol. Pharmaceutics* 12 (9), 3214–3225.
- (4) Silva, R., Vilas-Boas, V., Carmo, H., Dinis-Oliveira, R. J., Carvalho, F., de Lourdes Bastos, M., and Remião, F. (2015) Modulation of P-Glycoprotein Efflux Pump: Induction and Activation as a Therapeutic Strategy. *Pharmacol. Ther.* 149, 1–123.
- (5) U.S. Food and Drug Administration (2020) Clinical Drug Interaction Studies — Study Design, Data Analysis, and Clinical Implications Guidance for Industry, <https://www.fda.gov/downloads/drugs/guidances/ucm292362.pdf>.
- (6) European Medicines Agency (2012) Guideline on the investigation of drug interactions, [http://www.ema.europa.eu/docs/en\\_GB/document\\_library/Scientific\\_guideline/2012/07/WC500129606.pdf](http://www.ema.europa.eu/docs/en_GB/document_library/Scientific_guideline/2012/07/WC500129606.pdf).

- (7) Muzi, M., Mankoff, D. A., Link, J. M., Shoner, S., Collier, A. C., Sasongko, L., and Unadkat, J. D. (2009) Imaging of Cyclosporine Inhibition of P-Glycoprotein Activity Using  $^{11}\text{C}$ -Verapamil in the Brain: Studies of Healthy Humans. *J. Nucl. Med.* 50 (8), 1267–1275.
- (8) Kreisl, W. C., Liow, J. S., Kimura, N., Seneca, N., Zoghbi, S. S., Morse, C. L., Herscovitch, P., Pike, V. W., and Innis, R. B. (2010) P-Glycoprotein Function at the Blood-Brain Barrier in Humans Can Be Quantified with the Substrate Radiotracer  $^{11}\text{C}$ -N-Desmethyl-Loperamide. *J. Nucl. Med.* 51 (4), 559–566.
- (9) Savolainen, H., Cantore, M., Colabufo, N. A., Elsinga, P. H., Windhorst, A. D., and Luurtsema, G. (2015) Synthesis and Preclinical Evaluation of Three Novel Fluorine-18 Labeled Radiopharmaceuticals for P-Glycoprotein PET Imaging at the Blood-Brain Barrier. *Mol. Pharmaceutics* 12 (7), 2265–2275.
- (10) Savolainen, H., Windhorst, A. D., Elsinga, P. H., Cantore, M., Colabufo, N. A., Willemsen, A. T., and Luurtsema, G. (2017) Evaluation of [ $^{18}\text{F}$ ]MC225 as a PET Radiotracer for Measuring P-Glycoprotein Function at the Blood-Brain Barrier in Rats: Kinetics, Metabolism, and Selectivity. *J. Cereb. Blood Flow Metab.* 37 (4), 1286–1298.
- (11) Hildebrandt, I. J., Su, H., and Weber, W. A. (2008) Anesthesia and Other Considerations for in Vivo Imaging of Small Animals. *ILAR J.* 49 (1), 17–26.
- (12) Momosaki, S., Hatano, K., Kawasumi, Y., Kato, T., Hosoi, R., Kobayashi, K., Inoue, O., and Ito, K. (2004) Rat-PET Study without Anesthesia: Anesthetics Modify the Dopamine D1 Receptor Binding in Rat Brain. *Synapse* 54 (4), 207–213.
- (13) Tai, Y. F. (2004) Applications of Positron Emission Tomography (PET) in Neurology. *J. Neurol., Neurosurg. Psychiatry* 75 (5), 669–676.
- (14) Caruana, E. J., Roman, M., Hernández-Sánchez, J., and Solli, P. (2015) Longitudinal Studies. *J. Thorac. Dis.* 7 (11), E537–40.
- (15) Lubberink, M. (2016) Kinetic Models for Measuring P-Glycoprotein Function at the Blood-Brain Barrier with Positron Emission Tomography. *Curr. Pharm. Des.* 22 (38), 5786–5792.
- (16) Liow, J.-S., Kreisl, W., Zoghbi, S. S., Lazarova, N., Seneca, N., Gladding, R. L., Taku, A., Herscovitch, P., Pike, V. W., and Innis, R. B. (2008) P-Glycoprotein Function at the Blood-Brain Barrier Imaged Using  $^{11}\text{C}$ -N-Desmethyl-Loperamide in Monkeys. *J. Nucl. Med.* 50 (1), 108–115.
- (17) Mansor, S., Boellaard, R., Froklage, F. E., Bakker, E. D. M., Yaqub, M., Voskuyl, R. a., Schwarte, L. a., Verbeek, J., Windhorst, A. D., and Lammertsma, A. (2015) Quantification of Dynamic  $^{11}\text{C}$ -Phenytin PET Studies. *J. Nucl. Med.* 56 (9), 1372–1377.
- (18) Pottier, G., Marie, S., Goutal, S., Auvity, S., Peyronneau, M.-A., Stute, S., Boisgard, R., Dolle, F., Buvat, I., Caille, F., and Tournier, N. (2016) Imaging the Impact of the P-Glycoprotein (ABCB1) Function on the Brain Kinetics of Metoclopramide. *J. Nucl. Med.* 57 (2), 309–314.
- (19) Auvity, S., Caillé, F., Marie, S., Wimberley, C., Bauer, M., Langer, O., Buvat, I., Goutal, S., and Tournier, N. (2018) P-Glycoprotein (ABCB1) Inhibits the Influx and Increases the Efflux of  $^{11}\text{C}$ -Metoclopramide across the Blood-Brain Barrier: A PET Study on Non-Human Primates. *J. Nucl. Med.*, 1609–1615.
- (20) Alstrup, A. K. O., and Smith, D. F. (2013) Anaesthesia for Positron Emission Tomography Scanning of Animal Brains. *Lab. Anim.* 47 (1), 12–18.
- (21) Ohba, H., Harada, N., Nishiyama, S., Kakiuchi, T., and Tsukada, H. (2009) Ketamine/Xylazine Anesthesia Alters [ $^{11}\text{C}$ ]MNPA Binding to Dopamine D 2 Receptors and Response to Methamphetamine Challenge in Monkey Brain. *Synapse* 63 (6), 534–537.
- (22) Silva-Rodríguez, J., García-Varela, L., López-Arias, E., Domínguez-Prado, I., Cortés, J., Pardo-Montero, J., Fernández-Ferreiro, A., Ruibal, A., Sobrino, T., and Aguiar, P. (2016) Impact of Benzodiazepines on Brain FDG-PET Quantification after Single-Dose and Chronic Administration in Rats. *Nucl. Med. Biol.* 43 (12), 827–834.
- (23) McCormick, P. N., Ginovart, N., and Wilson, A. A. (2011) Isoflurane Anaesthesia Differentially Affects the Amphetamine Sensitivity of Agonist and Antagonist D2/D3 Positron Emission Tomography Radiotracers: Implications for in Vivo Imaging of Dopamine Release. *Mol. Imaging Biol.* 13 (4), 737–746.
- (24) Arakawa, R., Farde, L., Matsumoto, J., Kanegawa, N., Yakushev, I., Yang, K.-C., and Takano, A. (2018) Potential Effect of Prolonged Sevoflurane Anesthesia on the Kinetics of [ $^{11}\text{C}$ ]Raclopride in Non-Human Primates. *Mol. Imaging Biol.* 20 (2), 183–187.
- (25) Li, C. X., Patel, S., Auerbach, E. J., and Zhang, X. (2013) Dose-Dependent Effect of Isoflurane on Regional Cerebral Blood Flow in Anesthetized Macaque Monkeys. *Neurosci. Lett.* 541, 58–62.
- (26) Li, C.-X., Patel, S., Wang, D. J. J., and Zhang, X. (2014) Effect of High Dose Isoflurane on Cerebral Blood Flow in Macaque Monkeys. *Magn. Reson. Imaging* 32 (7), 956–960.
- (27) Schlünzen, L., Cold, G. E., Rasmussen, M., and Vafae, M. S. (2006) Effects of Dose-Dependent Levels of Isoflurane on Cerebral Blood Flow in Healthy Subjects Studied Using Positron Emission Tomography. *Acta Anaesthesiol. Scand.* 50 (3), 306–312.
- (28) Chi, O. Z., Hunter, C., Liu, X., and Weiss, H. R. (2010) The Effects of Isoflurane Pretreatment on Cerebral Blood Flow, Capillary Permeability, and Oxygen Consumption in Focal Cerebral Ischemia in Rats. *Anesth. Analg.* 110 (5), 1412–1418.
- (29) Greene, S. A. (2010) Anesthesia for Patients with Neurologic Disease. *Top. Companion Anim. Med.* 25 (2), 83–86.
- (30) Sijbesma, J. W. A., Zhou, X., Váñez García, D., Houwertjes, M. C., Doorduyn, J., Kwizera, C., Maas, B., Meerlo, P., Dierckx, R. A., Slart, R. H. J. A., Elsinga, P. H., and van Waarde, A. (2016) Novel Approach to Repeated Arterial Blood Sampling in Small Animal PET: Application in a Test-Retest Study with the Adenosine A1 Receptor Ligand [ $^{11}\text{C}$ ]MPDX. *Mol. Imaging Biol.* 18 (5), 715–723.
- (31) Fan, J., and de Lannoy, I. A. M. (2014) Pharmacokinetics. *Biochem. Pharmacol.* 87 (1), 93–120.
- (32) Váñez García, D., Casteels, C., Schwarz, A. J., Dierckx, R. A. J. O., Koole, M., and Doorduyn, J. (2015) A Standardized Method for the Construction of Tracer Specific PET and SPECT Rat Brain Templates: Validation and Implementation of a Toolbox. *PLoS One* 10 (3), e0122363.
- (33) Elmenhorst, D., Aliaga, A., Bauer, A., and Rosa-Neto, P. (2012) Test-Retest Stability of Cerebral mGluR5 Quantification Using [ $^{11}\text{C}$ ]ABP688 and Positron Emission Tomography in Rats. *Synapse* 66 (6), 552–560.
- (34) Landis, J. R., and Koch, G. G. (1977) The Measurement of Observer Agreement for Categorical Data. *Biometrics* 33 (1), 159.
- (35) Tiepolt, S., Hesse, S., Patt, M., Luthardt, J., Schroeter, M. L., Hoffmann, K.-T., Weise, D., Gertz, H.-J., Sabri, O., and Barthel, H. (2016) Early [(18F)]Florbetaben and [(11C)]PiB PET Images Are a Surrogate Biomarker of Neuronal Injury in Alzheimer's Disease. *Eur. J. Nucl. Med. Mol. Imaging* 43 (9), 1700–1709.
- (36) Liang, K.-Y., and Zeger, S. L. (1986) Longitudinal Data Analysis Using Generalized Linear Models. *Biometrika* 73 (1), 13–22.